

Influence of intrinsic point defects and substitutional impurities (Cl, I \rightarrow S) on the electronic structure of 2H-SnS₂

D.I. Bletskan, V.V. Frolova

Uzhhorod National University, 54, Voloshin Str., 88000 Uzhhorod, Ukraine
E-mail: crystal_lab457@yahoo.com

Abstract. It was performed the systematic investigation of chemical modification regularities of electronic structure at the composition changes of “ideal” 2H-SnS₂ crystal by using the self-consistent density functional theory method in the supercell model. It was analyzed the phases obtained during doping the sulfur sublattice by substitutional impurity Y \rightarrow S (Y = Cl, I) as well as during changing tin disulfide structure due to the appearance of atomic vacancies in cation and anion sublattices (non-stoichiometry effects).

Keywords: tin disulfide, electronic structure, density of states, intrinsic and extrinsic point defects, photoconductivity.

doi: <https://doi.org/10.15407/spqeo21.04.345>
PACS 61.72.J-, 61.72.-y, 71.38.-k, 72.40.+w

Manuscript received 17.10.18; revised version received 02.11.18; accepted for publication 29.11.18; published online 03.12.18.

1. Introduction

Tin disulfide (SnS₂) belongs to the family of layered semiconductors, which characteristic feature is the presence of polytypism. It is known more than 30 various SnS₂ polytypes, among which 2H, 4H and 18R base structures, are the most stable [1]. Crystal structures of all tin disulfide polytypes are formed by S–Sn–S three-layer packets (sandwiches), each of which is constructed by hexagonal monolayers of S and Sn atoms and has the trigonal symmetry. The SnS₂ polytypes with larger lattice constants c than for 4H-SnS₂ have some laying sequences of three-layer packets, which are the packing combinations of 2H/18R and 4H/18R base structures. They are not the simple variants of layer packing that allowed by geometry, but certainly, they are definitely intermediate ones between the base structures [2, 3].

In early papers, for example Ref. [4], the authors started description of the crystal structure for various polytypes of tin disulfide and designation of their space groups by the packing geometry of completely occupied

hexagonal layers combined in the molecular sandwiches S–Sn–S. However, it was found that 2H-SnS₂ has a significant difference between the measured and theoretically calculated density values using X-ray diffraction data ($\rho_{\text{meas.}} = 3.4 \text{ g/cm}^3$ is much less than $\rho_{\text{theor.}} = 4.32 \text{ g/cm}^3$) [2]. This difference of the measured and calculated densities is associated with the fact that only 79% positions of hexagonal Sn-monolayers and only 72% positions of S-monolayers of 2H-polytype crystal structure are filled. Thereof, it can be concluded that cation and anion vacancies are the dominant intrinsic point defects in 2H-SnS₂ crystals. Predominant formation of anion vacancy is caused by lower energy consumption for the break of only one of six covalent-ionic sulfur-tin bonds in [SnS₆] octahedron, while formation of cation vacancy requires additional breaks of much more covalent bonds of removed tin atom with tin atoms of its second coordination sphere. Consequently, real 2H-SnS₂ crystals always contain a large amount of intrinsic point (zero-dimensional) Schottky defects (anion V_S and cation V_{Sn} vacancies). Anion and cation vacancies in 2H-SnS₂

form the defect centers that play the role of electron traps and recombination centers, and thus they significantly affect the photoconductivity and photoluminescence of these crystals. However, the overwhelming majority of papers did not consider the non-stoichiometric effects when studying the physicochemical properties of $2H$ - SnS_2 crystals.

As shown by the authors of Ref. [2, 3], the important role in formation one or another polytype types during crystal growth from the gas phase by using the chemical transport reaction (CTR) method (except of temperature and vapor pressure in the crystallization zone) also plays the role of transport agent (carrier), which generally affects the chemical composition and first of all on stoichiometry. The growth of tin disulfide single crystals by CTR method usually leads to the doping of initial material by transporter atoms. In the vast majority of cases, halogens (Cl, I) are used as the transporting agents, and entering into the crystal they form another type of point defects – substitutional impurities Cl, $\text{I} \rightarrow \text{S}$ that significantly affects the resistivity [5–8].

Since the basic properties of solids (including crystals with defects) are determined by their electronic structure, the better understanding of optical, electrical, photoelectrical and photoluminescent properties of real defective $2H$ - SnS_2 crystals requires to ascertain changes in the band structure of ideal crystal that are caused by defects generating the localized states in the band gap. The important role in the study of electronic structure of defective crystals is played by the computational modeling, which allows not only to interpret the experimental data but also to predict them. Thus, it is evident that electronic structure calculations of real defective SnS_2 crystals can be very useful both for description of their fundamental electronic properties and to find the compositions possessing useful practical perspectives.

By now, the electronic structure and nature of interatomic interactions for stoichiometric defect-free SnS_2 crystal are fairly well studied [9–20]. As for the study of influence of intrinsic and impurity point defects on the electronic structure of tin disulfide, then we are not aware of this kind of papers.

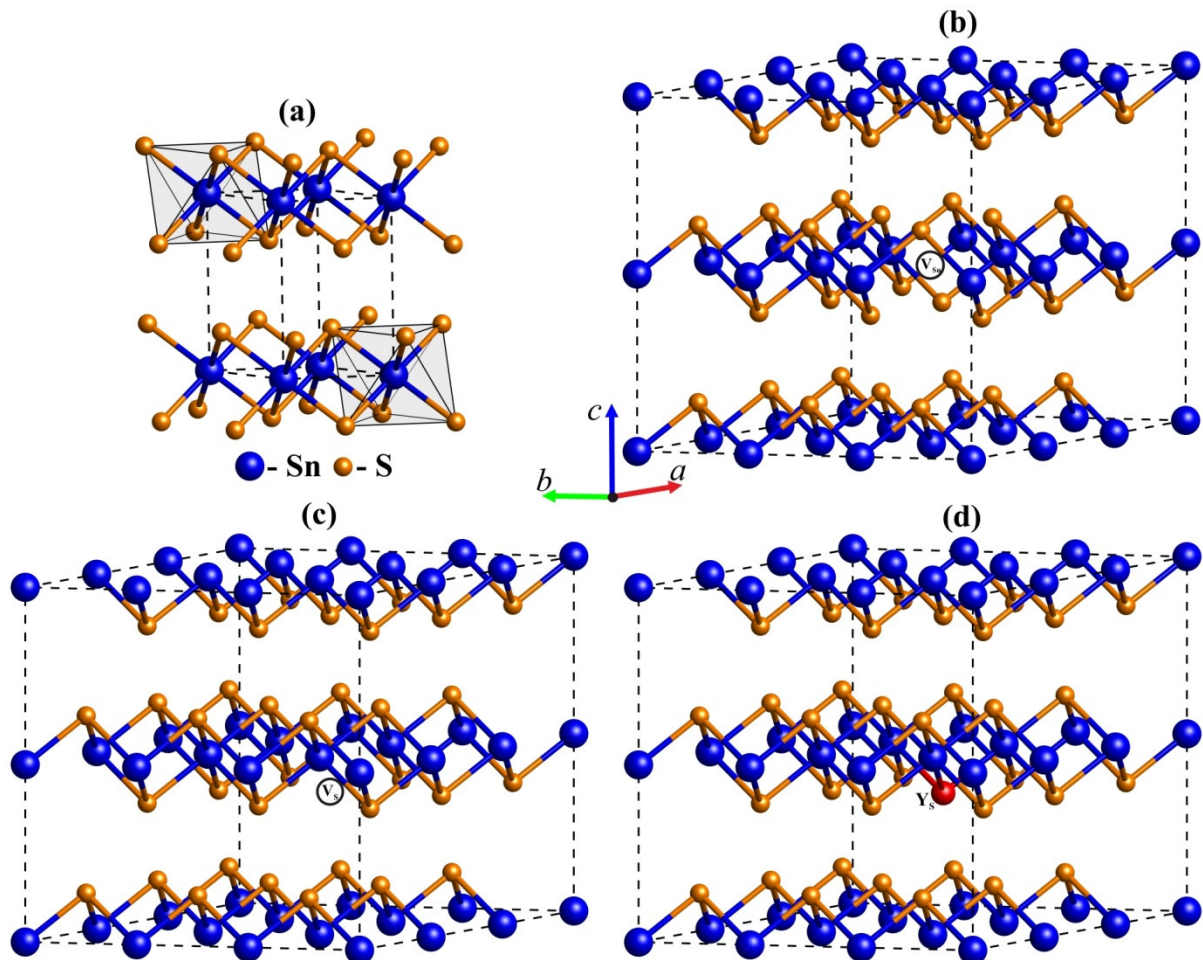


Fig. 1. Unit cell of $2H$ - SnS_2 (a), $3 \times 3 \times 2$ supercells of $2H$ - SnS_2 with tin (b), sulfur (c) vacancies and $\text{Y} \rightarrow \text{S}$ ($\text{Y} = \text{Cl}, \text{I}$) substitutional impurity (d).

This paper presents electronic structure calculations of defect-free tin disulfide crystal as well as the crystals containing intrinsic point defects (cation and anion vacancies) and isolated substitutional impurity atoms $Y \rightarrow S$ ($Y = \text{Cl}, \text{I}$), which are performed by *ab initio* density functional theory method in the LDA+ U approximation with accounting the single-site Coulomb correlations.

2. Crystal structure of 2H-SnS₂

2H-polytype of SnS₂ is characterized by CdI₂-type structure based on the three-layer packets (“sandwiches”), which are parallel to (001) plane. Each three-layer packet consists of a tin atom monolayer sandwiched between two close-packed monolayers of sulfur atoms (Fig. 1a). In the 2H-SnS₂ crystal structure, tin atoms are centered in the octahedra, which vertices are occupied by S atoms (Fig. 1a). The [SnS₆] octahedra are linked among themselves by common edges and form the three-layer –S–Sn–S– packets.

Bonds have the ion-covalent character within three-layer packets and bonds between three-layer packets are mainly performed by the van der Waals forces, it causes the large anisotropy of physical properties of 2H-SnS₂ crystals. Formation of various polytypes of tin disulfide depends on the layered character of three-layer packets along c axis. The layer packing order of the simplest 2H-SnS₂ structure is $[A\gamma B, A\gamma B]$, where γ designates tin atom monolayer and A, B – sulfur monolayers. The symmetry of 2H-polytype crystal lattice is characterized by the space group D_{3d}^3 ($P\bar{3}m_1$). Experimental parameters of crystal lattice are $a = b = 3.647 \text{ \AA}$, $c = 5.899 \text{ \AA}$, $\gamma = 120^\circ$ [2]. The equilibrium lattice parameters $a = b = 3.678 \text{ \AA}$, $c = 5.834 \text{ \AA}$, $\gamma = 120^\circ$ were used in the calculations, which we obtained at the total energy minimum of defect-free crystal modeling.

The unit cell of 2H-polytype contains three atoms. If the usual coordinate system is used, the unit cell of 2H-SnS₂ is described by two vectors \mathbf{a}_1 and \mathbf{a}_2 in the XY plane with the angle 120° between them as well as \mathbf{a}_3 vector along Z direction, and it contains the Sn atom located in Wyckoff position $\mathbf{a}(0, 0, 0)$ and two sulfur atoms located in Wyckoff position $\mathbf{d}(1/3, 2/3, z)$ with coordinates $(1/3, 2/3, u)$, $(2/3, 1/3, w)$, where $u = 0.25$, $w = 0.75$ before relaxation and $u = 0.25623$, $w = 0.74377$ after relaxation. The symmetry of specified positions is described by local groups $\bar{3}m$ and $3m$, respectively.

3. Calculation method

The presence of defects disturbs the translational symmetry of an ideal crystal. At the present time, the supercell model with *ab initio* calculation methods is most effectively used for the description of electronic structure of defective crystals.

This modeling was performed within the frames of density functional theory (DFT) method [21, 22] with the local density approximation (LDA) as an exchange-correlation functional. It is known that first-principle calculations within the density functional theory in the local density approximation for exchange-correlation potential give the underestimated values of band gap widths and defect centers depths. The LDA+ U method [23, 24] is used for more correct description of electronic correlation in comparison with LDA calculations. It is known that the magnitude of direct Coulomb single-site interaction U can significantly affect the depth of defect states in the band gap, and also the charge localization degree.

Calculations were performed using SIESTA software package [25, 26], which has a powerful and effective mechanism for the model manipulations of crystal unit cells: introduction and removal of atoms, formation of defects, introduction of distortions into the lattice, supercell construction and their relaxation, *etc.* In the supercell model, the infinite crystal is considered by introduction of periodic boundary conditions and a quasi-molecule is considered in the form of extended unit cell constructed using several primitive unit cells. This approach combines the advantages of molecular model (not all one-electron states of a crystal are considered but their finite number) with the correct consideration of the symmetry of object and does not create the problems associated with an extraction of fragment from the crystalline environment. Being mainly aimed at the electronic structure calculation of defective crystals, this method is also useful for the studying of band structures of defect-free crystals. The 54-atom supercell (Sn₁₈S₃₆) was produced for the modeling of stoichiometric tin disulfide as well as anion and cation vacancies. It was received by $3 \times 3 \times 2$ translation of 2H-SnS₂ unit cell, then the appearance of cation (V_{Sn}) or anion (V_{S}) vacancies was simulated by removing one of Sn or S atoms, respectively. Such cell $\{\text{Sn}_{17}\text{V}_{\text{Sn}}\text{S}_{36}\}$ corresponds to a cation-defective tin disulfide with a formal stoichiometry of Sn_{0.944}S₂. It must be emphasized that the supercell model supposed the ordered vacancy distribution in the crystal volume, given by the regular translation of supercell.

The geometry optimization procedure to minimize the supercell mechanical tensions was performed, which was considered as full-performed, when the force acting on each individual ion appeared is less than 0.01 eV/Å. Displacements caused by the presence of tin and/or sulfur vacancies change the bond lengths, but do not change the shape of local arrangement of the nearest and following upon the nearest atoms. So, in the case of cation vacancy presence, all six sulfur ions of the nearest vacancy environment undergo the significant shifts, moving from their regular positions in the direction from vacancy. The shift of S atoms from cation vacancy is explained by the fact that tin ion removal leads to the repulsion between S ions nearest to the vacancy and by Coulomb attraction of these sulfur ions toward tin ions of the second coordination sphere. The removal of S atom causes the shifts of surrounding Sn atoms in the direction from the vacancy.

4. Results and discussion

4.1. Electronic structure of defect-free 2H-SnS₂

As the first step of study, we performed the electronic structure calculations of defect-free SnS₂ crystal. The electronic structure of defect-free 2H-SnS₂ calculated using the density functional method without regard for the spin-orbital interaction in the LDA+U approximation in all high-symmetry points and directions of the Brillouin zone (Fig. 2) of hexagonal lattice is shown in Fig. 3a. The energy origin is set to the upper occupied level.

The valence band of defect-free 2H-SnS₂ (total width 13.11 eV) includes eight occupied bands. Layered character of 2H-SnS₂ crystal is reflected in the energy spectrum structure. It is observed the significant anisotropy of dispersion law for individual bands along and across three-layer packets. So, the dispersion of most of upper valence bands in the $\Gamma \rightarrow M$, $\Gamma \rightarrow K$ directions (along three-layer packet) exceeds the dispersion in the $\Gamma \rightarrow A$ direction (across layers). Weak dispersion $E(\mathbf{k})$ along the c axis of 2H-SnS₂ crystal (*i.e.*, along the $\Gamma \rightarrow A$ direction, which is perpendicular to the monolayers formed by Sn and S atoms) indicates the layered nature of compound and the relatively weak influence of interaction between three-layer packets on the electronic structure. The noticeable dispersion of bands along the directions parallel to the three-layer packets indicates the strong interaction in the structural [SnS₆] units, which form the sandwiches. These structure features of layered 2H-SnS₂ allow to tell about quasi-two-dimensional character of electronic energy spectrum.

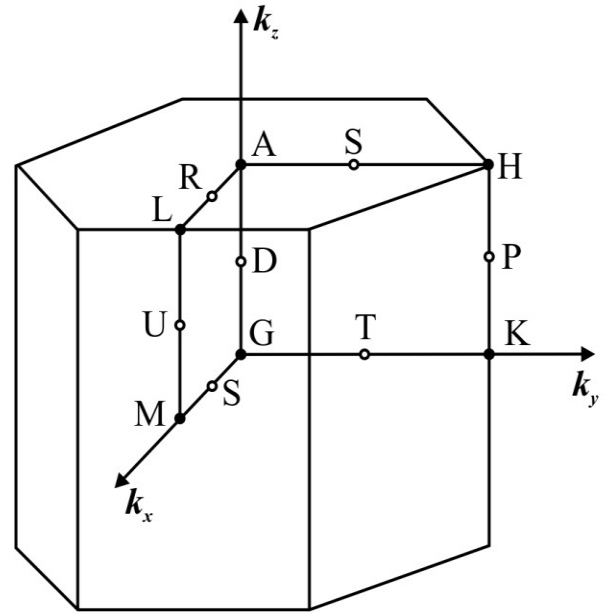


Fig. 2. Brillouin zone of 2H-SnS₂.

The calculations of total and local partial densities of states give information on the atomic orbital contributions into the crystal states of 2H-SnS₂. The spectra of total $N(E)$ and local partial $n_{at}(E)$ densities of electronic states (DOS) obtained on the basis of band calculation are shown in Fig. 3b. It is possible to identify the genetic origin of various subbands of occupied states by the analysis of partial contributions into the electronic density of states. The relationships between intensities of maxima in partial densities of states with various symmetry types are different. Partial sulfur s -, p -states predominate in the valence band of tin disulfide, and also their energy positions are significantly different. The coincidence of energy positions for the main maxima in the partial spectra of sulfur s -, p -states with the positions of corresponding maxima of tin s -, p -states indicates their strong hybridization.

Two lowest quasi-core bands (forming the valence band bottom) in the energy range from -13.11 to -10.38 eV are mainly formed by S $3s$ -atomic orbitals with the insignificant impurities of tin $5s$ -, $5p$ -states. The next subband in the energy range from -7.18 to -4.22 eV is formed by hybridized Sn $5s$ - and S $3p$ -orbitals, and contributions of these states are comparable in their magnitude. Formation of an intermolecular chemical bond is genetically associated with these bands. The energy gap between the middle of the occupied band and two bottom valence bands is 3.2 eV. The upper bunch of 5 occupied bands with 5.02 eV width has a mixed character involving the hybridized $3p$ -states of sulfur and $5p$ -states of tin. The uppermost part of this occupied

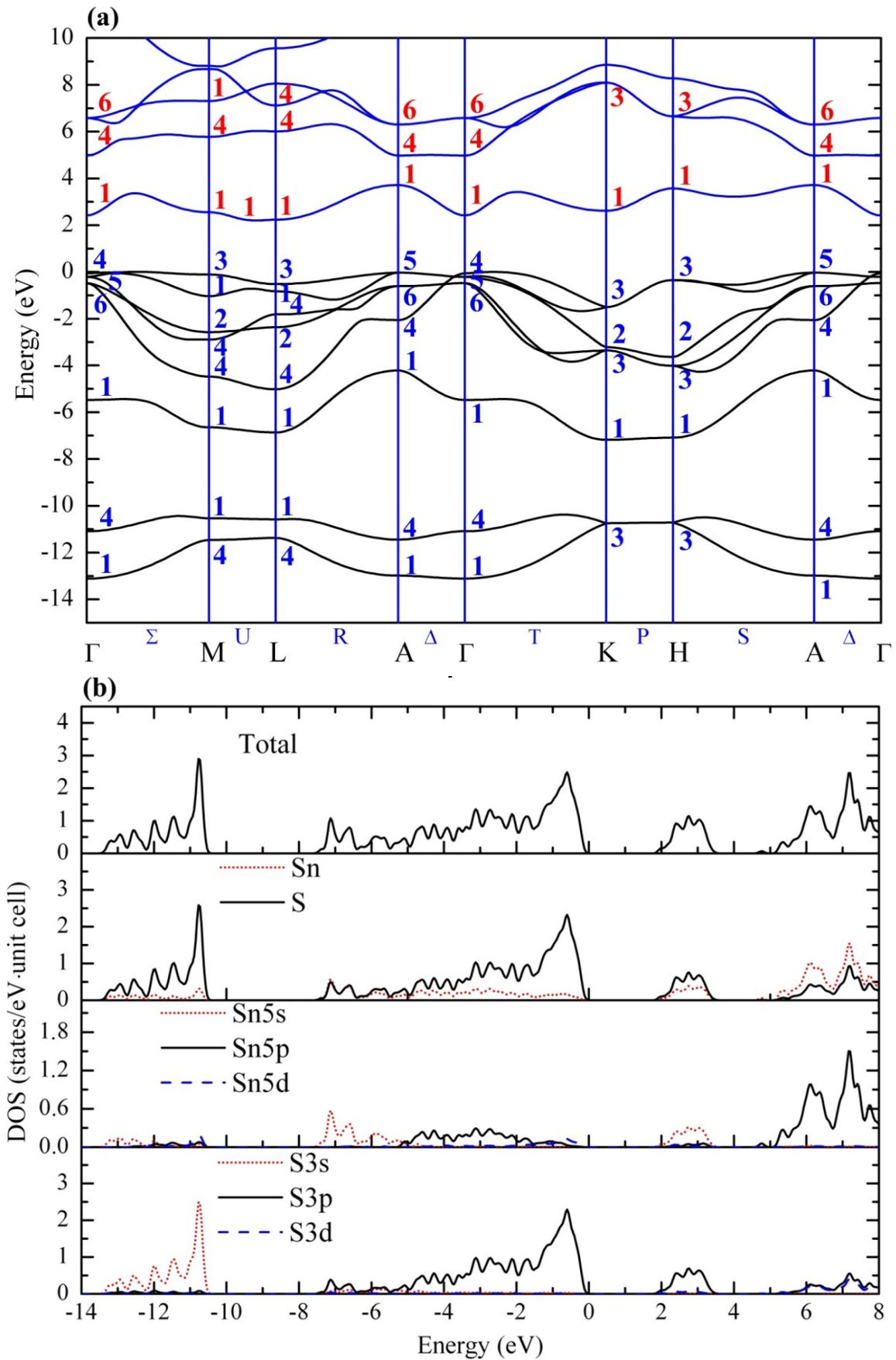


Fig. 3. Electronic structure (a), total and partial densities of states (b) of 2H-SnS₂ calculated using the LDA+U approximation.

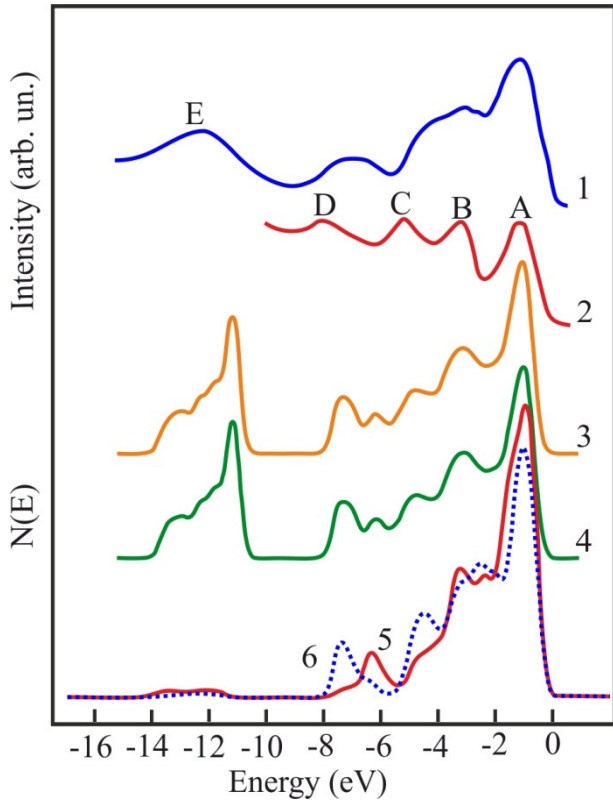


Fig. 4. Experimental XPS (1486 eV) [30] (1), UPS (22 eV) [31] (2) spectra of $2H\text{-SnS}_2$; calculated $2H\text{-SnS}_2$ total density of valence states in the unit cell (3) and supercell (4) models; partial densities of valence electronic p_z - (5) $p_{x,y}$ - (6) states of sulfur.

subband (1.5 eV width) has mainly anionic character, and sulfur p_z -states form its top.

The characteristic feature of $2H\text{-SnS}_2$ electronic structure is the presence of forbidden gap with 1.51 eV width in the conduction band separating the isolated low-energy unoccupied subband from the continuous spectrum of free states. This isolated subband of conduction band has significant dispersion and contains contributions of free Sn s -, S p -states. Free p -states of tin are dominating in the continuous spectrum of conduction band with the admixing of sulfur p -states.

According to the calculation results, $2H\text{-SnS}_2$ is an indirect-gap semiconductor with the valence band top located in the Γ point (Γ_4 symmetry) formed primarily by sulfur p_z -states. The conduction band bottom is localized in U direction (U_1 symmetry) of Brillouin zone. Our results are in good agreement with previously calculation data performed by the local pseudopotential method [14]. The value of indirect gap calculated in the LDA+ U approximation is $E_{gi} = 2.21$ eV (transition $\Gamma_4 \rightarrow U_1$), and it is close to the experimental values $E_{gi} = 2.21$ [27], 2.22 [28], 2.29 eV [29] obtained from the analysis of fundamental absorption spectra of $2H\text{-SnS}_2$ single crystals grown from the gas phase.

A necessary condition to compare the results of “defective” supercells is the reliable transfer of bulk properties of a defect-free crystal by the supercell model. For this purpose, we performed the electronic structure calculations of defect-free $2H\text{-SnS}_2$ crystal in the supercell model in the LDA+ U approximation (Fig. 5a).

The energy band structure of defect-free $2H\text{-SnS}_2$ crystal calculated by the density functional method in the $3 \times 3 \times 2$ supercell model is shown in Fig. 5a where the Fermi level is taken as the zero energy. For the band structure calculations of defect-free and defective crystals in the supercell model, we used only four high-symmetric points of the Brillouin zone, namely: $\Gamma(0, 0, 0)$, M (0.5, 0, 0), L(0.5, 0, 0.5), K(0.33, 0.33, 0), however, in order to ascertain the reliability of the results, some calculations were tested using six points. It follows from the comparison of electronic structures and density of states of defect-free $2H\text{-SnS}_2$ crystal calculated using the unit-cell (Figs. 3a and 3b) and by supercell (Figs. 5a and 5b) models that they do not significantly differ both by quantity of subbands as well as by their formation genesis.

The adequacy of the model description of electronic structure of defect-free $2H\text{-SnS}_2$ in the supercell approximation is determined by the similarity of calculated spectra of total density of states and experimental photoelectron spectra. The smoothed spectrum of total density of states $N(E)$ of defect-free tin disulfide calculated using the supercell model is compared in Fig. 4 in the unified energy scale with the known experimental X-ray and ultraviolet photoelectron spectra of $2H\text{-SnS}_2$ crystal taken from Refs. [30, 31]. It can be seen from this figure that the calculated $N(E)$ spectrum well reproduces the positions of gravity centers (centroids) of energy bands in the experimental XPS and UPS spectra. It is conditionally possible to allocate the A_1, A_2, A_3 subbands having the symmetry of p -orbital of sulfur in the binding energy range from 0 to 5 eV. The energy distribution of chalcogen $p_{x,y,z}$ -states in the occupied part of valence band is anisotropic (curves 5, 6, Fig. 4) which is the reflection of two-dimensional nature of $2H\text{-SnS}_2$ crystal structure.

4.2. Influence of intrinsic point defects on the electronic structure and density of states of $2H\text{-SnS}_2$ crystal

The electronic structure of $2H\text{-SnS}_2$ crystal with intrinsic point defects (tin (V_{Sn}) and sulfur (V_{S}) vacancies) is presented by the band diagram in Fig. 5. It is important for the analysis of electronic structure of defective crystal to separate the states related with the presence of defects from the states typical for the crystal matrix.

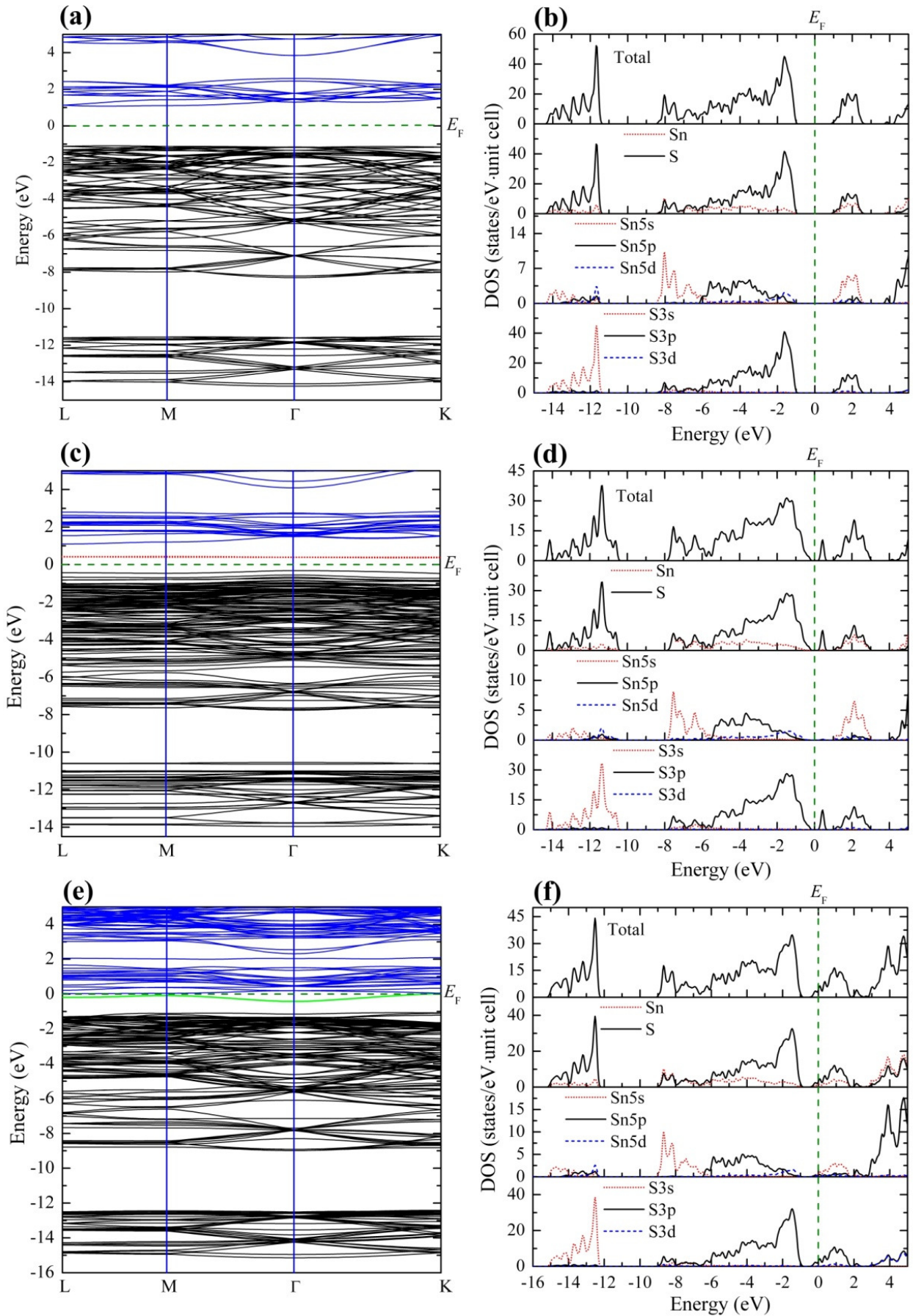


Fig. 5. Electronic structure, total and partial densities of states of defect-free $2H\text{-SnS}_2$ (a, b) as well as $2H\text{-SnS}_2$ with cation (c, d) and anion (e, f) vacancies calculated in $3\times 3\times 2$ supercell model.

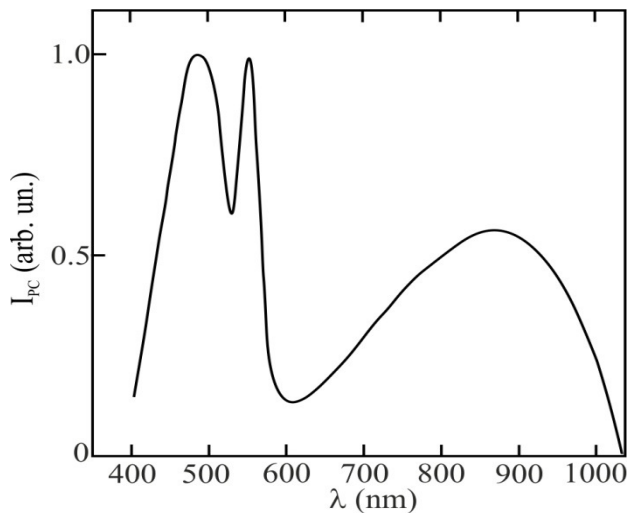


Fig. 6. Photoconductivity spectra of $2H\text{-SnS}_2$ crystal. $T = 293$ K.

The presence of cation vacancy in $2H\text{-SnS}_2$ crystal leads not only to modification of crystal local geometry, but it also primarily reflects the electronic properties of whole crystal system as well as, in particular, of ions near the defect. Cation vacancies in $2H\text{-SnS}_2$ induce the appearance of an intense peak of density of states in the depth of valence band in the pseudo-gap region above the quasi-core sulfur $3s$ -subband. The genesis of these cation vacancy states (generally of sulfur s -symmetry) is caused by restructuring the electronic states of matrix, where the wave functions of sulfur atoms nearest to the cation vacancy play the decisive role. Important changes also occur in the middle subband of occupied states, where S $3p$ -Sn $5s$ -hybridization takes place. The nature of these changes is manifested in restructuring the peak intensities in the partial DOS-spectrum of tin $5s$ -states which is a reflection of bond changes (more precisely their breaks, absence) in that part of $[\text{SnS}_6]$ octahedra that have no tin atoms, *i.e.*, there are cation vacancies. Besides, in the band spectrum of non-stoichiometric $2H\text{-SnS}_2$ above the valence band top there is the acceptor level, which nature is associated with sulfur $3p$ -states.

The coordination number of tin atom in $2H\text{-SnS}_2$ is greater than that of sulfur atom. Consequently, formation of anion vacancies in $2H\text{-SnS}_2$ crystals is caused by the lower energy costs of the breaking one of six ion-covalent sulfur-tin bonds in the $[\text{SnS}_6]$ octahedron in comparison with the energy costs for formation of cation vacancy. Therefore, in the case of non-stoichiometric $2H\text{-SnS}_2$ with anion vacancies the density of occupied states practically does not undergo the significant changes in comparison with a defect-free crystal; at the same time, the donor level appears in the fundamental gap of band spectrum, its nature is related with the mixed S $3p$ - and

Sn $5p$ -states (Fig. 5f). In the case of LDA modeling, the donor level practically overlaps with the conduction band bottom, whereas accounting the Hubbard correlation (U) within the LDA approximation gives the defective level by 0.47 eV away from the bottom of conduction band (Fig. 5f). The approximately flat form of dispersion law curve for the donor level indicates the strong localization in the real space. Thus, it can be concluded from the obtained calculation data that anion vacancy plays a role of deep donor in tin disulfide.

Intrinsic point defects, being electrically charged, significantly affect the electrical, photoelectrical and photoluminescent properties of $2H\text{-SnS}_2$ crystals. Since V_{Sn} vacancies create the acceptor levels in the band gap and V_{S} – donor levels, the crystals grow up the self-compensated, and they are high-resistance by this reason; the concentration of anion vacancies in $2H\text{-SnS}_2$ crystals prevails over the concentration of cation vacancies, in vast majority of cases they have the n -type conductivity. The intensive impurity band with a maximum 875 nm (1.42 eV), observed in the photoconductivity spectrum (Fig. 6) behind the intrinsic absorption edge, testifies the presence of high concentration of intrinsic point defects in $2H\text{-SnS}_2$ crystals, which we grown by the sublimation method. Besides, two more intrinsic high-energy bands are observed in the photoconductivity spectra, which nature is related with the band-to-band transitions. So, the band with a maximum 2.25 eV (550 nm) is caused by the indirect transitions $\Gamma_4 \rightarrow U_1$ from the valence band to the conduction band (Fig. 3) and the more high-energy maximum 2.55 eV (485 nm) is caused by the direct optical transitions $\Gamma_4 \rightarrow \Gamma_1$. These results of studying the PC spectra of $2H\text{-SnS}_2$ crystals well agree with the spectra given in Ref. [32, 33], which in addition to the intrinsic bands also contain the intense impurity band near 900 nm [32] (865 nm [33]).

4.3. Influence of Cl, I \rightarrow S substitutional impurities on the electronic structure of $2H\text{-SnS}_2$.

The main changes of energy spectrum associated with the structural vacancies have been already considered above. The Cl, I \rightarrow S substitutional impurities are another type of zero-dimensional defects in $2H\text{-SnS}_2$ crystals, grown using CTR method. The concentrations of these mentioned defects in the anion sublattice depending on the growing conditions and the concentrations of transporting agent in the growth ampoule can reach the very significant values in real crystals (up to 10^{17} cm^{-3}), which can significantly change the physical properties [7]. It requires to study the influence of these impurities on the energy spectrum of an initial matrix.

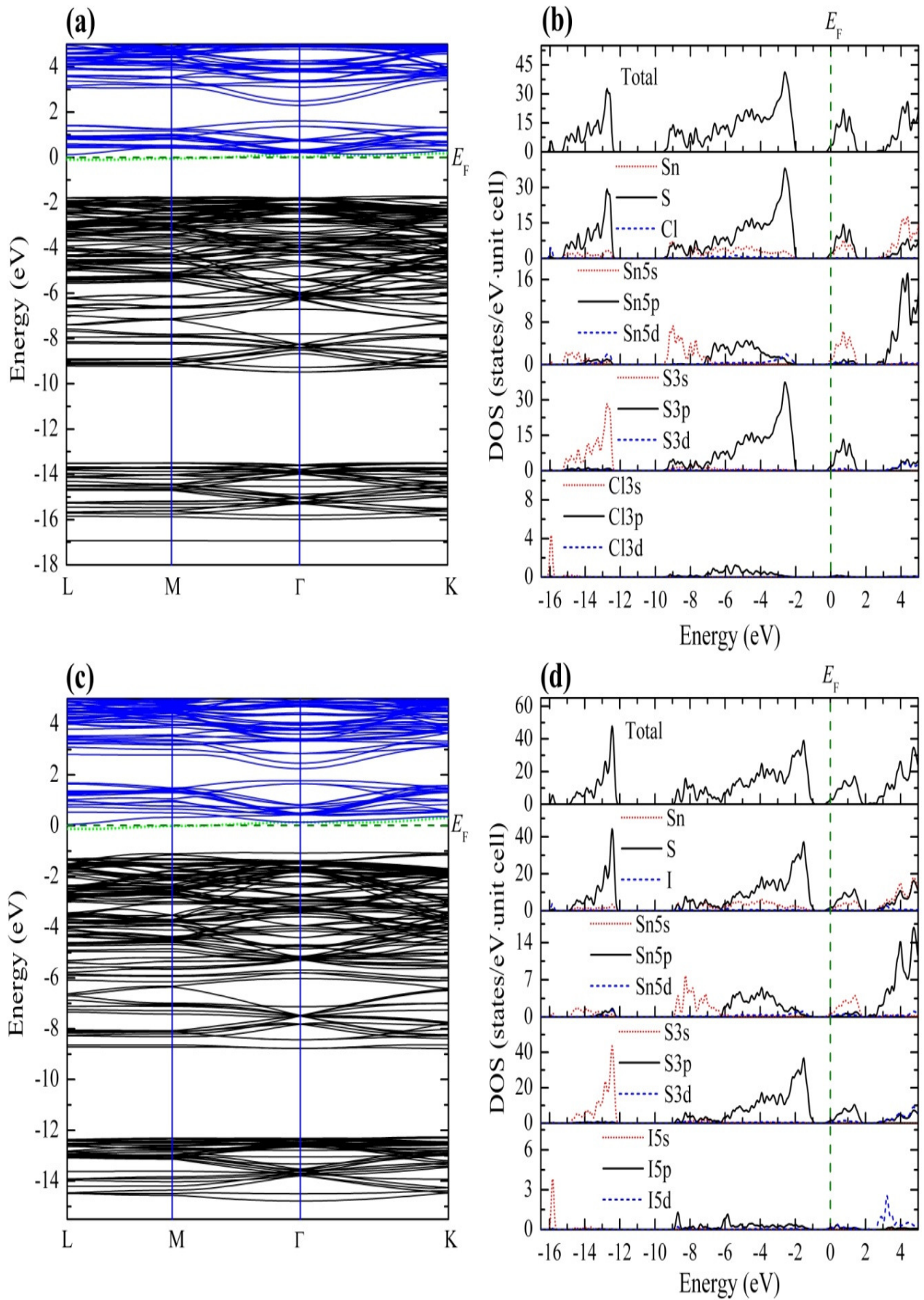


Fig. 7. Electronic structure, total and partial densities of states of $2H\text{-SnS}_2$ crystal with anion substitutional impurity Cl (a, b), I (c, d) in $3\times 3\times 2$ supercell model.

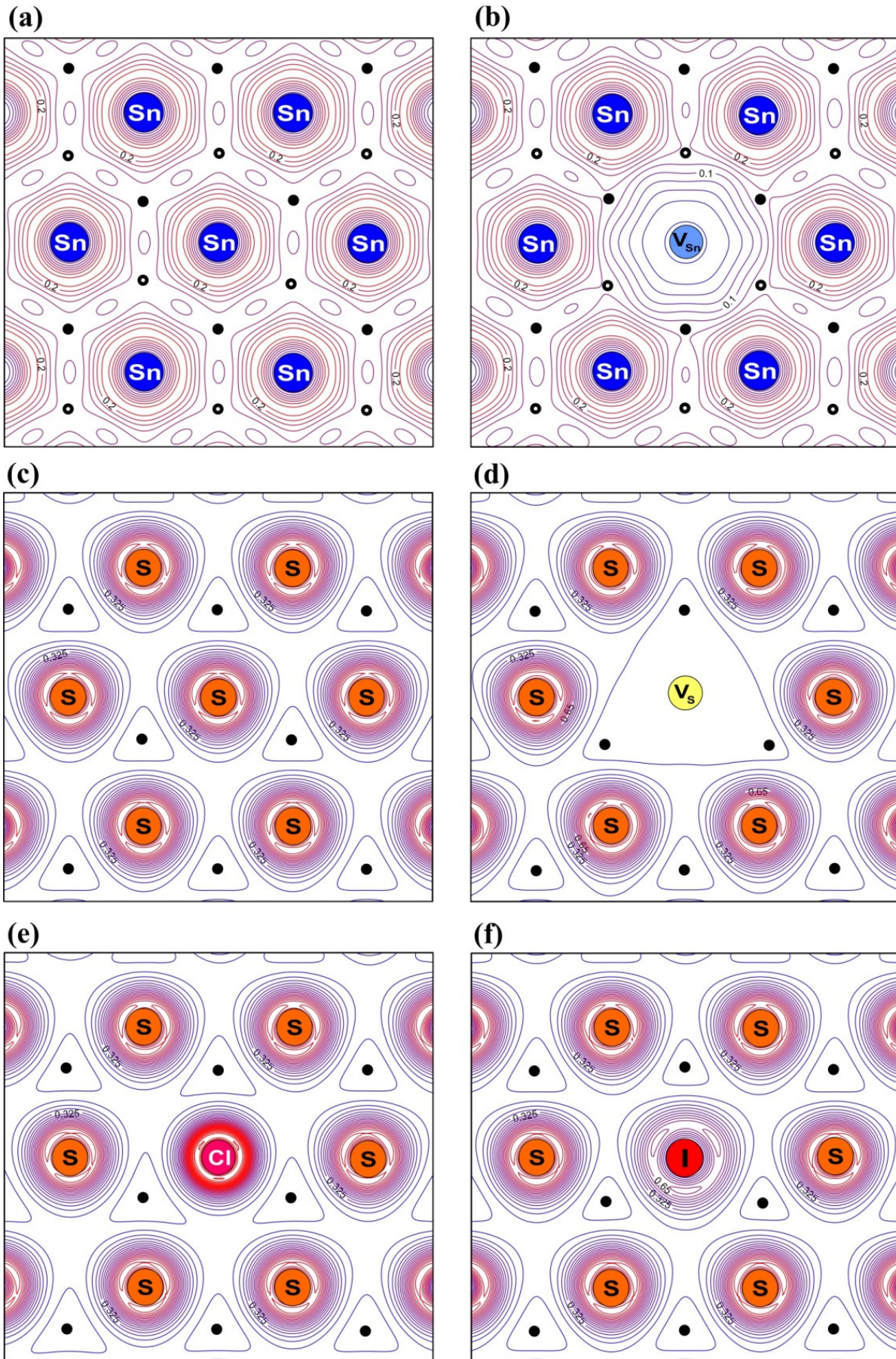


Fig. 8. Electronic density distribution maps of defect-free $2H\text{-SnS}_2$ crystal (a, c) as well as $2H\text{-SnS}_2$ with cation (b), anion (d) vacancies and Cl, I \rightarrow S substitutional impurities (e, f) in the cation (a, b) and anion (c-f) sublattice planes.

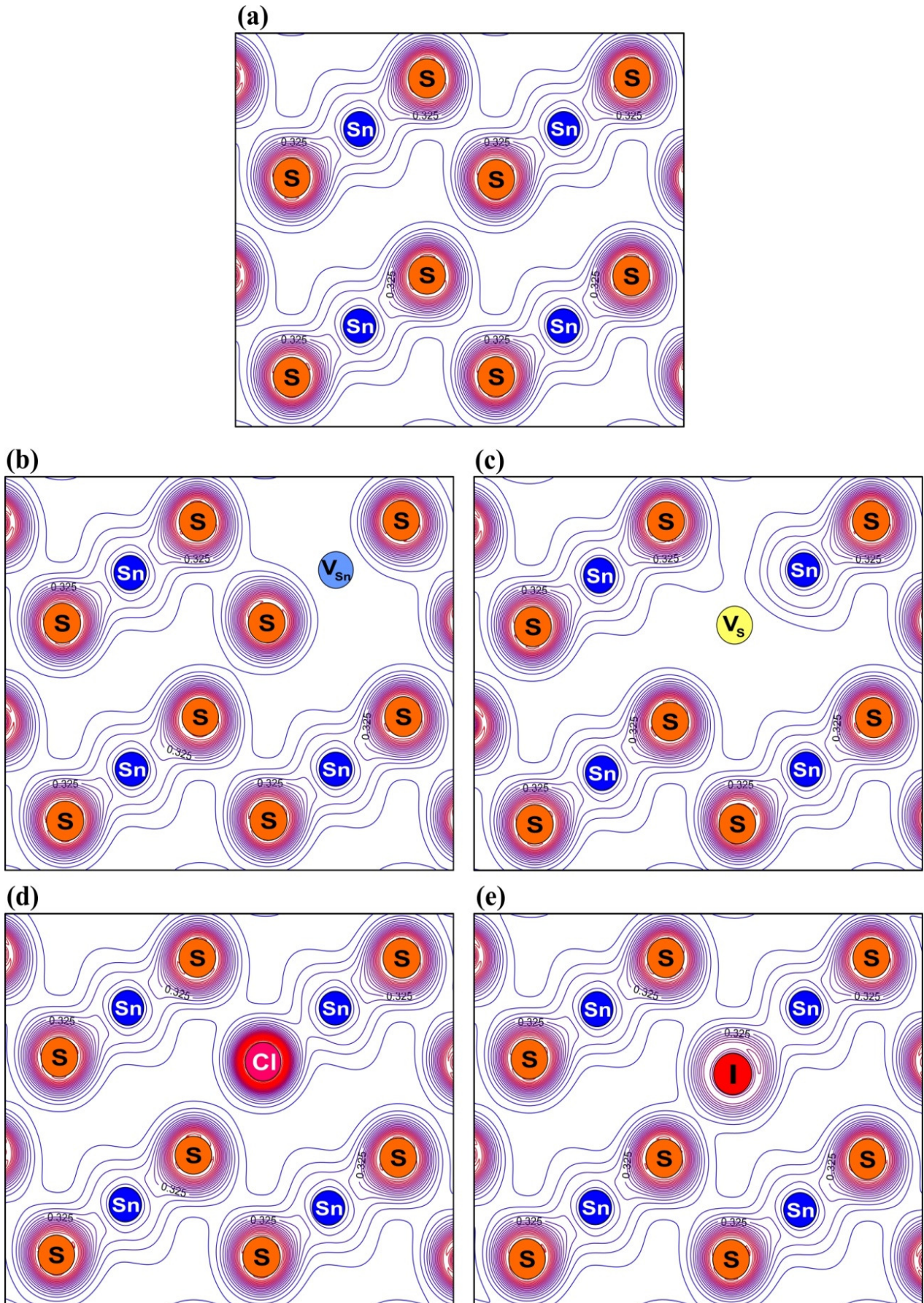


Fig. 9. Electronic density distribution maps of defect-free $2H\text{-SnS}_2$ crystal (a) as well as $2H\text{-SnS}_2$ with V_{Sn} cation (b), V_{S} anion (c) vacancies and Cl, I \rightarrow S substitutional impurities (d, e) in the (110) plane.

In the vast majority of cases, the interaction of impurity atoms with the matrix lattice leads to modification of impurity atom potential and to formation of deep levels in the energy spectrum of crystal. The energy positions of impurity levels depend on how well the impurity atoms entered into the electronic and geometrical structure of the main lattice, *i.e.*, it is determined by the impurity atom locations in the lattice, their dimensions and structures of electronic shells. The same factors determine the limited solubility of impurities in these crystals [34]. From the crystallochemical point of view, with account of atom sizes (the covalent radii are 1.40 Å for Sn, 1.03 Å for S, 1.07 Å for Cl, 1.345 Å for I [35]) and electronegativities, chlorine and iodine should preferably occupy the sites in the S sublattice. It strongly depends on the number of valence electrons in the impurity and substituted atoms, whether the substitutional impurity will behave as a donor or as an acceptor. Halogen atoms (Cl, I) with seven electrons in the external shell replacing sulfur with six electrons exhibit a donor action; the doping of tin disulfide by these impurities during crystal growth by using the CTR method leads to formation of crystals with a high concentration of electrons $\sim 10^{20} \text{ cm}^{-3}$ [36]. The losses of chlorine (iodine) during the post-growth annealing do not change the initial *n*-type of conductivity, since sulfur vacancies represent the donor centers.

The hybridization degree of wave functions of single impurity centers with the crystal valence states is determined by their mutual energy position. Electronic structure calculations in the $\text{Sn}_{18}\text{S}_{35}\text{Y}_1$ supercell (Fig. 7) show that substitution of sulfur atoms with the halogen ones leads to appearance of deep energy levels in the energy spectrum below the S 3*s*-band that corresponds to the electronic *s*-states localized on the chlorine (iodine) atoms as well as on the nearest tin atoms. The analysis of spectra of local partial states of impurity atoms shows that *p*-states of halogen atoms participate in formation of middle and upper valence subbands. It testifies appearance of chemical bonds between impurity and tin atoms. It is possible to destiny on the nature of this bond from the spatial distribution of electronic charge density between tin and impurity atoms (Figs. 9d and 9e).

Besides, introduction of substitutional impurity atoms ($\text{Y} \rightarrow \text{S}$, $\text{Y} = \text{Cl, I}$) leads to appearance of local donor-type levels in the band gap of 2*H*- SnS_2 crystal near the conduction band bottom (Fig. 7); their depth increases in the Cl \rightarrow I series, which qualitatively agree with the values obtained from the temperature dependence of electrical conductivity of crystals grown using the CTR method (Cl, I transporter) [36]. In the

same impurity series, it is observed the systematic decrease of static Mulliken charge value on the halogen atom, which correlates with the electronegativity value decrease during the transition from chlorine to iodine.

4.4. Electronic density distribution in 2*H*- SnS_2 crystals with intrinsic and impurity point defects

The mechanism of chemical bonding formation in the defect-free and defective tin disulfide can be analyzed in detail by consideration of electronic density contour maps constructed on the basis of DFT calculations in the supercell model. Electronic charge distribution between different tin (sulfur) atoms belonging to the same cation (anion) monolayer in a three-layer packet is presented by the maps shown in Figs. 8a and 8c. Solid lines on contour maps describe the surfaces of constant electronic density, and the density of lines in the figures describes the gradient of electronic density. The positions of S atoms in the monolayer located above (the distance 1.49 Å or 1/4*c*) the tin monolayer plane are designated in Fig. 8a by the points, and S atoms located below this plane are designated by the circles. The nearest neighbors of S atom are three Sn atoms (designated by the points in Fig. 8c) which are at the equal distances. It can be seen from Figs. 8a and 8c that there are no common lines of $\rho(r)$ level for the neighboring cations (anions) in tin (sulfur) monoatomic layers, which indicates a weak overlap of their wave functions.

Fig. 9 shows the electronic density maps inside the three-layer packets, reflecting the chemical bonding of tin atoms with the nearest neighbor sulfur atoms in $[\text{SnS}_6]$ octahedra. Valence density distribution in the anion-cation plane passing along Sn–S bonds in $[\text{SnS}_6]$ octahedra (Fig. 9) reveals the presence of common contour lines between cation (Sn) and anion (S) (it indicates hybridization of Sn 5*s*-, 5*p*- and S 3*s*-, 3*p*-states). At the same time, it is observed the polarization of an electronic cloud in the direction from S atom to Sn atom. The electronic density gradient is directed along Sn–S bonds with primary density localization on sulfur atoms due to their higher electronegativity. The strongly pronounced deformation of $\rho(r)$ contours from sulfur atoms toward tin atoms along the Sn–S bond line as well as the presence of common contours encompassing the maxima of electron density over the cation-anion bonds characterize the covalent component of the chemical bond in three-layer packets. The presence of covalent component in SnS_2 is caused by hybridization of sulfur 3*p*-states and tin 5*s*-, 5*p*-states (Fig. 5). The charge of covalent bond is responsible for the stability of $[\text{SnS}_6]$ octahedral structural units in this compound.

Ionic component of chemical bond is caused by the partial transfer of charge density between tin and sulfur atoms due to the difference of their electronegativities ($EN^{\text{Sn}} = 1.96$, $EN^{\text{S}} = 2.58$). It is reflected on the electronic density maps by the greater density of valence electrons near the localization places of sulfur atoms as well as by the charge reduction on the covalent bond between sulfur and tin atoms.

It can be seen from Fig. 9 that the electronic density within the three-layer packets is much higher than near their boundaries. The charge distribution in a single three-layer packet forms an almost closed shell that indicates a weak interpacket van der Waals interaction caused by sulfur p_z -states that partially enter into the interlayer space. This spatial anisotropy of electronic density and energy distribution of electronic sulfur $3p$ -states is the reason for quasi-two-dimensionality of tin disulfide crystals.

Thus, the interatomic interactions in the defect-free SnS_2 have the combined character and include covalent, ionic and van der Waals components of chemical bond.

Since deviation from the stoichiometric composition and the presence of impurity Cl, I atoms affect the physical and chemical properties of layered $2H\text{-SnS}_2$ crystals, so it is important to ascertain the chemical bond features in this compound with the presence of anion and/or cation vacancies as well as Cl, I \rightarrow S substitutional impurity. Changes of total charge density distribution caused by the anion (cation) removal and formation of vacancies or introduction of foreign substitutional atoms are also convenient to study with the charge density maps.

The presence of tin (sulfur) vacancies in $2H\text{-SnS}_2$ layered crystals is illustrated by the $\rho(r)$ charge density distribution maps in tin (sulfur) atomic grids (Figs. 8b and 8d). It can be seen that $\rho(r)$ distribution in the vacancy (V_{Sn} , V_{S}) localization places has the delocalized character. Charge density deformation in the defective SnS_2 is visible in Figs. 8, 9: there are no new Sn–Sn (S–S) bonds passing through the vacancy center, and the charge density contour deformations reflect its growth along Sn–Sn bond line near the defect.

According to the form of total charge distribution, it is possible to note that the electronic density perturbation in the presence of (V_{Sn} , V_{S}) cation (anion) vacancies is experienced by the atoms at least of two its coordination spheres. This effect is demonstrated by the isoelectronic maps of non-stoichiometric SnS_2 (Fig. 9). The vacancy perturbing the acting mechanism is associated with the changes of electronic states of sulfur atoms nearest to V_{Sn} . It occurs the transfer of a part of S $3p$ -states to the region of non-bonding states. As a result of the presence

of tin vacancies, it occurs the “emptying” of the parts of bonding states, the Fermi level shifts down on the energy scale, and the density of states near E_F increases.

Introduction of chlorine and iodine atoms into sulfur position of tin disulfide does not lead to the changes in the general mechanism of interatomic interactions. Contours $\rho(r)$ near impurity Cl (I) atoms testify the presence of covalent component of Sn–Cl(I) bond (Fig. 9). The main role of covalent bond effects between Cl(I) impurity and nearest tin atoms is played by Cl(I) p –Sn p -interactions. The defining one is the bonding between tin and introduction Cl, I elements, having p – p -type.

It is observed the systematic decrease of static Mulliken charge on the halogen atom (Cl – 7.350 e , I – 7.189 e) in the impurity Cl \rightarrow I series, which correlates with the decrease of electronegativity values during the transition from chlorine to iodine (Cl – 3.16, I – 2.66). When sulfur is replaced with chlorine (iodine), the length of $R_{\text{Sn-Cl(I)}} = 2.76 \text{ \AA}$ (2.96 \AA) regularly increases in comparison with $R_{\text{Sn-S}} = 2.60 \text{ \AA}$. It should be noted that the difference in sizes of impurity and tin atoms leads to the appearance of local elastic deformations in the vicinity of crystalline lattice sites occupied by the impurity atoms.

Estimates of population changes of separate bond types (Sn–Sn, Sn–S) allow to confirm that the near covalent Sn–S bonds of s , p – p -type remain as the main interaction type in both complete (stoichiometric) and defective compositions.

5. Conclusions

For the first time within the density functional theory, it was study the influence of tin (V_{Sn}) and sulfur (V_{S}) lattice vacancies as well as substitutional impurities ($Y \rightarrow \text{S}$, $Y = \text{Cl, I}$) on the electronic spectrum and chemical bonding of $2H\text{-SnS}_2$. Quantum-chemical calculations have shown that the presence of vacancies in tin disulfide crystal structure leads to changes of its electronic structure and formation of defective states in the band gap. Thus, in the case of V_{Sn} cation vacancy it occurs the acceptor level in the band gap separated from the valence band top on 0.3 eV; in the case of V_{S} sulfur vacancy it occurs the donor level separated from the conduction band bottom on 0.47 eV. Introduction of chlorine and iodine atoms into tin disulfide does not lead to changes in the general mechanism of interatomic interactions in this compound. Bonding between tin and introduction elements (Cl, I) remains crucial and are s , p – p -type. Bonding between non-metallic components (S–Cl, S–I) is absent.

References

- Bletskan D.I. *Crystalline and Glassy Chalcogenides of Si, Ge, Sn and Alloys on Their Basis*, Vol. 1. Uzhhorod, Zakarpattia, 2004.
- Palosz B., Steurer W. and Schulz H. Refinement of SnS₂ polytypes 2H, 4H and 18R. *Acta Cryst. B*. 1990. **46**. P. 449–455.
- Palosz B. and Salje E. Lattice parameters and spontaneous strain in AX₂ polytypes: CdI₂, PbI₂, SnS₂ and SnSe₂. *J. Appl. Crystallography*. 1989. **22**. P. 622–623.
- Whitehouse C.R. and Balchin A.A. Polytypism in tin disulfide. *J. Cryst. Growth*. 1979. **47**. P. 203–212.
- Kourtakis K., DiCarlo J., Kershaw R., Dwight K. and Wold A. Preparation and characterization of SnS₂. *J. Solid State Chem*. 1988. **76**. P. 186–191.
- Shibata T., Muranushi Y., Miura T. and Kishi T. Electrical characterization of 2H-SnS₂ single crystals synthesized by the low temperature chemical vapor transport method. *J. Phys. Chem. Solids*. 1991. **52**. P. 551–553.
- Conroy L. and Park K.C. Electrical properties of the group IV disulfides TiS₂, ZnS₂, HfS₂, and SnS₂. *Inorg. Chem*. 1968. **7**. P. 459–463.
- Said G. and Lee P.A. Electrical conduction mechanisms in tin disulphide. *phys. status solidi (a)*. 1973. **15**. P. 99–103.
- Fong C.Y. and Cohen M.L. Electronic energy-band structure of SnS₂ and SnSe₂. *Phys. Rev. B*. 1972. **5**. P. 3095–3101.
- Schlüter I.Ch. and Schlüter M. The electronic structure of SnS₂ and SnSe₂. *phys. status solidi (b)*. 1973. **57**. P. 145–155.
- Mula G. and Aymerich F. Electronic structure of SnS₂. *phys. status solidi (b)*. 1972. **51**. P. K35–K37.
- Murray R.B. and Williams R.H. Band structure and photoemission studies of SnS₂ and SnSe₂: II. Theoretical. *J. Phys. C*. 1973. **6**. P. 3643–3651.
- Robertson J. Electronic structure of SnS₂, SnSe₂, CdI₂ and PbI₂. *J. Phys. C*. 1979. **12**. P. 4753–4766.
- Powell M.J., Marseglia E.A. and Liang W.Y. The effect of polytypism on the band structure of SnS₂. *J. Phys. C*. 1978. **11**. P. 895–904.
- Schlüter I.Ch. and Schlüter M. Electronic structure of SnS₂ and SnSe₂. *Helv. Phys. Acta*. 1973. **46**. P. 31.
- Schluter M. Band structure of GaSe. *Nuovo Cimento B*. 1973. **13**. P. 313–320.
- Aymerich F., Meloni F. and Mula G. Pseudopotential band structure of solid solutions SnS_xSe_{2-x}. *Solid State Commun*. 1973. **12**. P. 139–141.
- Aymerich F. and Mula G. Pseudopotential band structures of Mg₂Si, Mg₂Ge, Mg₂Sn, and of the solid solution Mg₂(Ge, Sn). *phys. status solidi (b)*. 1970. **42**. P. 697–704.
- Bordas J., Robertson J. and Jakobsson A. Ultraviolet properties and band structure of SnS₂, SnSe₂, CdJ₂, PbJ₂, BiJ₂ and BiOJ crystals. *J. Phys. C*. 1978. **11**. P. 2607–2621.
- Gonzalez J.M. and Oleynik I.I. Layer-dependent properties of SnS₂ and SnSe₂ two-dimensional materials. *Phys. Rev. B*. 2016. **94**. P. 125443–1–10.
- Hohenberg P. and Kohn W. Inhomogeneous electron gas. *Phys. Rev*. 1964. **136**. P. B864–B871.
- Kohn W. and Sham L.J. Self-consistent equations including exchange and correlation effects. *Phys. Rev*. 1965. **140**. P. A1133–A1138.
- Anisimov V.I., Zaanen J. and Andersen O.K. Band theory and Mott insulators: Hubbard U instead of Stoner I. *Phys. Rev. B*. 1991. **44**. P. 943–954.
- Anisimov V.I., Aryasetiawan F. and Lichtenstein A.I. First-principal calculations of the electronic structure and spectra of strongly correlated systems: the LDA+U method. *J. Phys*. 1997. **9**. P. 767–808.
- <http://icmab.cat/leem/siesta/>
- Soler J.M., Artacho E., Gale J.D., García A., Junquera J., Ordejón P. and Sánchez-Portal D. The SIESTA method for ab initio order-N materials simulation. *J. Phys*. 2002. **14**. P. 2745–2779.
- Greenaway D.L. and Nitsche R. Preparation and optical properties of group IV–VI₂ chalcogenides having the CdI₂ structure. *J. Phys. Chem. Solids*. 1969. **26**. P. 1445–1458.
- Lee P.E., Said G., Davis R. and Lim T.H. On the optical properties of some layer compounds. *J. Phys. Chem. Solids*. 1969. **30**. P. 2719–2729.
- Powell M.J. The effect of pressure on the optical properties of 2H and 4H-SnS₂. *J. Phys. C*. 1977. **10**. P. 2967–2977.
- Williams R.H., Murray R.B., Govan D.W., Thomas J.M. and Evans E.L. Band structure and photoemission studies of SnS₂ and SnSe₂: I. Experimental. *J. Phys. C*. 1973. **6**. P. 3631–3642.
- Margaritondo G., Rowe J.E., Schluter M. and Kasper H. Conduction and valence band density of states of SnS₂: theory and experiment. *Solid State Commun*. 1977. **22**. P. 753–757.
- Nakata R., Yamaguchi M., Zembutsu S. and Sumita M. Crystal growth and photoconductive effects of stannic chalcogenides. *J. Phys. Soc. Jpn*. 1972. **32**. P. 1153.

33. Patil S.G. and Tredgold R.H. Electrical and photoconductive properties of SnS₂ crystals. *J. Phys. D.* 1971. **4**. P. 718–722.
34. Milnes A.G. *Deep Impurities in Semiconductors*. New York, Wiley, 1973.
35. Pyykkö P. Refitted tetrahedral covalent radii for solids. *Phys. Rev. B.* 2012. **85**. P. 024115-1–7.
36. Bletskan D.I. and Frolova V.V. The influence method and conditions for growing on the electrical properties of SnS₂ crystals. *Naukovyi visnuk Uzhgorod. Natsional. Universitetu. Ser. Fyzyka.* 2015. **37**. P. 36–50 (in Ukrainian).

Authors and CV



Dmytro I. Bletskan. Doctor in Physics and Mathematics Sciences, Professor, professor of the department physics of semiconductors at Uzhhorod National University, Ukraine. Authored over 260 scientific publications, 86 patents, 2 textbooks, 2 monographs. The area of his scientific interests – technology and physics of highly anisotropic layered crystals, chalcogenide glassy semiconductors and superionics.

Uzhhorod National University



Viola V. Frolova. Researcher of the Institute for Solid State Physics and Chemistry (INPCSS) at Uzhhorod National University, Ukraine. Authored 30 scientific publications and 2 patents. The area of scientific interests is electronic structure and optical properties of layered crystals.

Uzhhorod National University